Calculations of the Elastic Constants of Crystals as Functions of Pressure with Applications to Quartz and Cristobalite

by

Hui Zhao

Thesis submitted to the Faculty of the
Virginia Polytechnic Institute and State University
in partial fulfillment of the requirements for the degree of

MASTER OF SCIENCE

in

Geological Sciences

APPROVED:

G.V. Gibbs, Co-Chairman

M.B. Boisen, Jr., Co-Chairman

M.F. Hochella

A.L. Ritter

May, 1994

Blacksburg, Virginia

Calculation of the Elastic Constants of Crystals

as Functions of Pressure

with Applications to Quartz and Cristobalite

by

Hui Zhao

(Abstract)

Assuming that its deformation is both static and homogeneous, a method was devised within the framework of finite strain theory to calculate the elastic constants of a crystal at zero pressure as well as functions of pressure. As this method can be used for a crystal of any symmetry with a variety of potentials, elastic constant calculations were completed for both quartz and cristobalite using the potentials derived by Lasaga and Gibbs (1987, 1988), Tsuneyuki et al. (1988), van Beest et al. (1990) and Boisen and Gibbs (1993). Among the four theoretical potentials derived from force fields calculated for molecule $H_6Si_2O_7$, two potentials associated with the SiO bond stretching as well as the OSiO and the SiOSi bond angle bending terms yield reasonable agreements with the experimental data, supporting the assumption that the binding forces in crystals are similar to those in small molecules (Gibbs 1982). Using the semi-empirical potentials, including the SQLOO potential derived with the covalent model (Boisen and Gibbs 1993) and two derived with the ionic model (Tsuneyuki et al. 1988; van Beest et al. 1990), calculations of the elastic constants reproduce the experimental results for both quartz and cristobalite. The pressure derivatives of the elastic constants calculated with these potentials also agree with the experimental results measured for quartz at low pressures and yield pressure derivatives of the bulk modulus that are in close agreement with that observed for quartz. Using

the SQLOO potential, although the results of the calculations do not agree with the experimental data as well as those calculated using the two ionic potentials, the agreement of the calculations made with the theoretical potentials was improved significantly. Finally, using the three semi-empirical potentials, the elastic constants were calculated as functions of pressure for quartz and cristobalite up to their transitional pressures. Calculated for both quartz and cristobalite, different behaviors of the elastic constants were found using different potentials. For cristobalite, the variations of its elastic constants and bulk modulus are better modeled by the SQLOO potential as its structural behaviors calculated with the SQLOO potential are consistent with the X-ray diffraction studies..

Acknowledgements

A lot of people I want to thank for their helps. First I would like to thank Dr. Gibbs and Dr. Boisen, who gave me the great opportunity to study in their group with the exciting project. I also want to thank them for their supports and encouragements during all the years I stay in Blacksburg. Also, I am grateful for the Department of Geological Sciences in accepting me into its graduate program. Indeed, my thanks go out to everybody in this department. Especially, I would like to express my most gratitude to Dr. Bloss, for his kindness, encouragements, and expectations that I owe so much. I also want to thank Dr. S. C. Shu and Hercules Incorporated for their financial supports at the first year I stayed in Blacksburg. Especially, I want to thank Dr. Shu for the helps he gave to me at the most miserable time of my life, and also Prof. Lin Shan at Eastchina Institute of Geology. The tragic death of Prof. Lin Shan I will regret all the times. Also, I want to thank my advisor for my undergraduate project, Prof. Zhenggang Zhang, who helped me get into the university and is the first one to bring me into the exciting area of mineral physics. Without the selfless helps of these people, I do not dare to image what my life would be.

I also want thank Dr. Hochella and Dr. Ritter to serve in my committee and provide valuable suggestions for this work. Prof. Rogers and Prof. Renardy in the department of mathematics are thanked for the help regarding the implicit function theory and Prof. Lee Johnson is thanked for his work on the minimization program MADMAX. I also want to thank everyone in my group. Especially, I want to thank Bob Downs, who gave me a lot of helps at the beginning of the project. Also with him, I shared so many simulating conversations about the excitingness of mineral physics.

Finally, I want to thank my parents for their supports. I am deeply sorry for

the hardship that I brought into their life.

The National Science Foundation is thanked for supporting this work through the grants EAR-9303589 awarded to G.V. Gibbs and M.B. Boisen.

Table of Contents

List of Figures

List of Tables

Introduction

Significant progress has been made during the last few years in the modeling of the structural and physical properties of crystals (See Catlow and Price 1990 and references therein). Usually in these models, interactions among the individual atoms are described either with empirical potentials that have been derived only from experimental results, or with semi-empirical potentials that have been derived from a combination of experimental and theoretical results, which were obtained from quantum mechanical calculations completed on small molecules, or with theoretical potentials that have been derived entirely from quantum mechanical calculations completed on small molecules. In principle, from these potentials, a variety of properties can be calculated for a material, including its crystal structures, elastic constants, vibrational spectra and also phonon dispersion curves. Up to this point in time, however, the majority of the calculations have been focusing on the studies of the structural behaviors of the materials. By comparison, few elastic constant calculations have been made. This is particularly the case for crystals with complex structure and low symmetry as the elastic constants are difficult to calculate for such crystals.

Nonetheless, as elasticity is one of the most important properties, attempts have been made by a number of workers to calculate the elastic constants of crystals. In most of the calculations, pairwise potentials have been employed to describe the Coulombic interactions, so that the elastic constants could be calculated using the codes developed by Catlow and his coworkers (Catlow and Mackrodt 1982). Using the empirically derived ionic shell model potentials with formal charges assumed on the ions, Price and Park (1987) and Sanders et al. (1984) found that they could reproduce the elastic constants of forsterite and quartz to within a few percent. More recently, Purton et al. (1993) modified the coefficients

of Sanders' potential to match the force field calculated for the molecule $H_{12}Si_5O_{16}$, and found that they could not only reproduce the elastic and dielectric constants for quartz, but also its phonon dispersion curves. After comparing the results calculated from their potential to those calculated from the potentials derived by others, they concluded that, in order to model the elastic and lattice dynamical properties of quartz accurately, inclusion of long range Coulombic forces is necessary. They also calculated the elastic constants of quartz as functions of pressure. With a correction for the effective elastic constants under pressure (Barron and Klein 1965), similar calculations have been completed for forsterite, quartz and albite by Wall et al. (1993). The results of these calculations, however, have not been reported for quartz and so could not be compared with the experimental data. Using the ionic model with partial charges assumed on the ions, Tsuneyuki et al. (1988) and van Beest et al. (1990) have derived two potentials separately from the quantum mechanical calculations completed on the SiO_4^{4-} ion and the H_4SiO_4 molecule, respectively. As the *ab initio* calculations alone are not sufficient to determine the potential energy functions, the experimental data of quartz were also incorporated in deriving these potentials. With the resulting potentials, the elastic constants of quartz could be reproduced to within 10% (van Beest et al. 1990; Purton et al. 1993).

In this study, the elastic constants of a crystal are calculated by assuming that its deformation is both static and homogeneous. The method proposed by Catti (1985, 1989a) is presented within the more rigorous framework of finite strain theory in this study. Unlike the strategies used by Catlow (Catlow and Mackrodt 1982) and others, Catti undertook a calculation of the elastic constants of a crystal in terms of the changes of its energy with respect the changes of the unit cell dimensions and the changes of the atomic coordinates. Thus, instead

of expressing the energy in terms of the interatomic distances, the strategy used by Catti (1985, 1989a) only requires a calculation of the energy per unit cell as a function of the cell dimensions and the atomic coordinates as well as the first and the second order derivatives of the energy function with respect to these variables. As such a calculation is straightforward and relatively easy to make, Catti's strategy can be used to calculate the elastic constants for a crystal of any symmetry and structure using a wide range of potentials. Furthermore, using finite strain theory, Catti's method is extended in this study to calculate the elastic constants of a crystal as functions of pressure.

Because of its abundance in nature as well as its technological importance, quartz has been the subject of numerous experimental studies. The elastic constants of quartz have been measured by McSkimin et al. (1965) up to $\sim$1 GPa. Recently, with the use of the rectangular parallellepiped resonance method, such data were also determined with improved accuracy by taking the piezoelectric effects into account (Ohno 1990). As the use of non-piezoelectric theory result in an overestimation of c_{11} by only 2σ and an underestimation of c_{12} by only σ, it can be concluded that earlier measurements of the elastic constants of quartz have been reasonably accurate. Hence, in the calculation of its elastic constants and their pressure derivatives at room conditions, the piezoelectric effect of quartz can be ignored without introducing serious errors. In this study, the elastic constants of quartz and cristobalite were calculated using the potentials derived by Lasaga and Gibbs (1987, 1988), Tsuneyuki et al. (1988), van Beest et al. (1990) and Boisen and Gibbs (1993). The results of these calculations were then compared with the experimentally determined data (McSkimin et al. 1965; Yeganeh-Haeri et al 1992). In addition, the elastic constants of quartz and cristobalite were calculated as functions of pressure up to their transitional pressures. Although it is

not clear to us whether the piezoelectric effects are important or not at high pressure, no such effects were included. For quartz, the resulting pressure derivatives of its elastic constants were compared with those measured at low pressures by McSkimin et al. (1965).

Definition of the elastic constants in the macroscopic regime

In our calculations, surface effects are eliminated by assuming that the crystal is infinite in extent and periodic. Since the crystal is also assumed to maintain its translational symmetry under static homogeneous deformations, each unit cell of the crystal will be treated as equivalent and having the same number of atoms and structure as the one located at the origin. If the representative cell contains N atoms, then the geometry of the unit cells and the positions of the atoms in each cell can be specified with only 3N+6 parameters, of which 6 define the unit cell dimensions and 3N define the fractional coordinates of the N atoms. The energy of the crystal can also be expressed as a function of the 3N+6 variables that define the structure of the crystal, as it is invariant under rigid rotations. Therefore, with a given potential, the energy of the crystal per unit cell can be expressed as

$$U = U(a_1, \cdots, a_6; x_1^{\,1}, \cdots, x_1^{\,3}, \cdots\cdots, x_N^{\,1}, \cdots, x_N^{\,3}) \tag{1}$$

where a_i, $i = 1, \cdots, 6$, denote the cell dimensions a, b, c, α, β, and γ, respectively and $x_i^{\,1}$, $x_i^{\,2}$, $x_i^{\,3}$, denote the fractional coordinates of the ith atoms, $i = 1, \cdots, N$. In addition, if one atom in the representative cell is fixed at the origin, then the number of independent variables that determine the energy can be further reduced to 3N+3.

According to the scheme used by Barron et al. (1971), the energy expression U can be considered to be given with respect to a general regime where both

the cell dimensions and the positional parameters of the atoms are treated as independent variables. Using the general regime, however, the elastic constants of a crystal can not be defined directly. In order to define the elastic constants, the deformation of the crystal must be specified first. From the atomic point of view, a deformation of a crystal is composed of two parts, the external strain describing the changes of its cell dimensions and the internal strain describing the atomic displacements. Macroscopically, the deformation of the crystal can be specified only with respect to the changes of its cell dimensions. Although not stated explicitly, an assumption is usually made that the individual atoms position themselves to minimize the energy of the crystal (Barron et al. 1971). Thus, in addition to the general regime, a macroscopic regime need also be introduced. In the macroscopic regime, as the atomic coordinates are treated as dependent variables with the equilibrium conditions

$$\frac{\partial U(a_1, \cdots, a_6; x_\mu{}^\alpha)}{\partial x_\mu{}^\alpha} = 0, \qquad \mu = 1, \cdots, N \quad \text{and} \quad \alpha = 1, \cdots, 3 \tag{2}$$

the energy of the crystal per unit cell can be expressed as a function

$$\hat{U} = \hat{U}(a_1, \cdots, a_6) \tag{3}$$

where only the cell dimensions are considered as independent variables.

In the macroscopic regime, if the coordinate systems are always chosen to be consistent with the translational symmetry of the crystal, then under a homogeneous deformation, the finite strain tensor can be defined as

$$\eta = \frac{1}{2}(\mathbf{G} - \bar{\mathbf{G}}) \tag{4}$$

where $\mathbf{G}$ is called the metrical tensor with its components calculated from the inner products of the base vectors $D = \{\mathbf{a}_1, \mathbf{a}_2, \mathbf{a}_3\}$. $\bar{\mathbf{G}}$ denotes the metrical tensor

associated with the reference configuration, which is often chosen as the state of the crystal before the deformation occurs in the Lagrangian representation. It need not, however, be the stress free state necessarily (Toupin and Bernstein 1961; Wallace 1965). Any initially stressed state of the crystal may also qualify as a reference configuration, provided that Eq.2 is satisfied with the finite deformation. Then evaluated at the initial state, the stress induced from the finite deformation can be calculated from the first order derivatives of the energy function $\hat{U}$ with respect to the strain tensor components η_{ij} as

$$T^{ij} = \frac{1}{V}\frac{\partial \hat{U}(a_1, \cdots, a_6)}{\partial \eta_{ij}} = \frac{2}{V}\frac{\partial \hat{U}(a_1, \cdots, a_6)}{\partial g_{ij}} \mid_{g_{ij}=\bar{g}_{ij}} \tag{5}$$

where $i, j = 1, \cdots, 3$ and V is the volume of the unit cell of the crystal at the initial state. Similarly, the elastic constants of the crystal defined at the initial state can be calculated from the second order derivatives

$$C^{ijkl} = \frac{1}{V}\frac{\partial^2 \hat{U}(a_1, \cdots, a_6)}{\partial \eta_{ij}\partial \eta_{kl}} = \frac{4}{V}\frac{\partial^2 \hat{U}(a_1, \cdots, a_6)}{\partial g_{ij}\partial g_{kl}} \mid_{g_{ij}=\bar{g}_{ij}, g_{kl}=\bar{g}_{kl}} . \tag{6}$$

As both the stress components and the elastic constants are defined in terms of the natural coordinate system, the upper indices are used to indicate that they are contravariant tensor components.

By using the chain rule in variable calculus, the stress components and the elastic constants defined by Eq.5 and Eq.6 can also be calculated directly from the derivatives of the energy function $\hat{U}$ with respect to the cell dimensions. To simplify the calculations, Voigt's notation will be used as the tensor components in Eq.5 and Eq.6 are symmetric with respect to the interchanges of their indices within each pair (Nye 1957). For the stress tensor components and the elastic constants, if each pair of their indices is abbreviated with the relation

$$\begin{array}{rcccccccccc} i,j & = & 11 & 22 & 33 & 32 & 23 & 31 & 13 & 12 & 21 \\ i & = & 1 & 2 & 3 & & 4 & & 5 & & 6, \end{array}$$

then they can be written directly into the elements of a 1×6 and a 6×6 matrix, respectively. Similar contractions can also be made for the strain tensor and the metrical tensor components, except that a factor 2 must be introduced for their shear components such as $g_i = g_{ii}$ for $i = 1, \cdots, 3$, $g_4 = 2g_{23} = 2g_{32}$, $g_5 = 2g_{31} = 2g_{13}$ and $g_6 = 2g_{12} = 2g_{21}$ for the metrical tensor components. Thus, with the Voigt's notation, Eq.5 and Eq.6 translate respectively into

$$T^i = \frac{2}{V} \sum_{p=1}^{6} \frac{\partial a_p}{\partial g_i} \cdot \frac{\partial \hat{U}}{\partial a_p} \tag{7}$$

and

$$C^{ij} = \frac{4}{V} \left(\sum_{p=1}^{6} \frac{\partial^2 a_p}{\partial g_i \partial g_j} \cdot \frac{\partial \hat{U}}{\partial a_p} + \sum_{p=1}^{6} \sum_{q=1}^{6} \frac{\partial a_p}{\partial g_i} \cdot \frac{\partial a_q}{\partial g_j} \cdot \frac{\partial^2 \hat{U}}{\partial a_p \partial a_q} \right) \tag{8}$$

where i and j range from 1 to 6. The quantities $(\partial a_p / \partial g_i)$ and $(\partial^2 a_{pq} / \partial g_i \partial g_j)$ are evaluated from the equations $g_{ij} = a_i a_j \cos(\mathbf{a}_i \cdot \mathbf{a}_j)$ at the initial state.

Calculations of the elastic constants in terms of the general regime

With a given potential function, the energy of a crystal per unit cell can not be expressed analytically as a function of the cell dimensions alone. In this study, as the derivatives of the energy function were calculated with the finite difference method, one way to calculate the derivatives of function $\hat{U}$ in the macroscopic regime is to minimize the energy function U with respect the atomic coordinates for each change in the cell dimensions. Using the SQLOO potential (Boisen and Gibbs 1993), the elastic constants of quartz were calculated in this manner. A better way to calculate the elastic constants, however, is to consider the general regime, in which the derivatives of function U can be calculated directly with respect to both the cell dimensions and the atomic coordinates. The expressions of the elastic constants in terms of these derivatives have been previously derived (Barron et al. 1971; Cousins 1978). Here, however, the discussion will be made in a mathematically more rigorous setting. Using the SQLOO potential, the elastic

constants of quartz calculated in the general regime agree with the calculation completed in the macroscopic regime up to the sixth decimal place.

In the general regime, the calculation of the elastic constants can be accomplished by considering the atomic coordinates as dependent variables of the cell dimensions as required by Eq.2. Due to the translational invariance of the energy function, however, these coordinates can not be determined uniquely in terms of the given cell dimensions. In order to express the atomic coordinates explicitly as functions of the cell dimensions, additional constraints are required. One frequently used method to introduce the extra constraints is to fix one of the atoms at the origin. So within one unit cell, only 3N-3 variables are needed to specify the positions of the atoms. However, because the fixed atom has to be treated differently from the rest in this treatment, it may be better to fix the frame of the reference instead.

In this approach, the frame of the reference is set by fixing the geometrical center of the crystal with the constraints

$$\sum_{\mu=1}^{N} x_{\mu}^{\alpha} = 0. \qquad \alpha = 1.\cdots, 3 \tag{9}$$

Then, together with Eq.2, there exist 3N+3 constraints. In order to apply the implicit function theory, three auxiliary variables, Z_α, $\alpha = 1, \cdots, 3$, are introduced by modifying Eq.2 to be

$$\frac{\partial U(a_1, \cdots, a_6, x_{\mu}^{\alpha})}{\partial x_{\mu}^{\alpha}} + Z_\alpha = 0. \qquad \mu = 1, \cdots, N \quad \text{and} \quad \alpha = 1, \cdots, 3 \tag{10}$$

As the translational invariance of the energy function U require these variables to equal zero with the equations

$$\sum_{\mu=1}^{N} \frac{\partial U}{\partial x_{\mu}^{\alpha}} = 0, \qquad \alpha = 1, \cdots, 3$$

the introduction of Z_α is only for mathematical convenience.

Using the implicit function theorem (Protter and Morrey 1977 pp-332), both $x_\mu^{\ \alpha}$ and Z_α can be considered locally as functions of $a_p, p = 1, \cdots, 6$ such as

$$x_\mu^{\ \alpha} = \hat{x}_\mu^{\ \alpha}(a_1, \cdots, a_6) \qquad \mu = 1, \cdots, N \quad \text{and} \quad \alpha = 1, \cdots, 3 \tag{11}$$

and

$$Z_\alpha = \hat{Z}_\alpha(a_1, \cdots, a_6). \qquad \alpha = 1, \cdots, 3 \tag{12}$$

Then with functions $\hat{x}_\mu(a_1, \cdots, a_6)$ and $\hat{Z}_\alpha(a_1, \cdots, a_6)$, both Eq.9 and Eq.10 must be satisfied for any given set of cell dimensions. By further differentiating Eq.9 and Eq.10 with respect to a_p, the following equations can be derived

$$\frac{\partial}{\partial a_p}\left(\frac{\partial U}{\partial x_\mu^{\ \alpha}}\right) + \sum_{\nu=1}^{N}\sum_{\beta=1}^{3} \frac{\partial}{\partial x_\nu^{\ \beta}}\left(\frac{\partial U}{\partial x_\mu^{\ \alpha}}\right) \cdot \frac{\partial \hat{x}_\nu^{\ \beta}}{\partial a_p} + \frac{\partial \hat{Z}_\alpha}{\partial a_p} = 0 \qquad p = 1, \cdots, 6 \tag{13}$$

and

$$\sum_{\mu=1}^{N} \frac{\partial \hat{x}_\mu^{\ \alpha}}{\partial a_p} = 0, \qquad p = 1, \cdots, 6 \tag{14}$$

which may also be written as

$$\left[\begin{array}{ccc|c} & \dfrac{\partial^2 U}{\partial x_\mu^{\ \alpha} \partial x_\nu^{\ \beta}} & & \begin{matrix} I \\ \vdots \\ I \end{matrix} \\ \hline I & \cdots & I & 0 \end{array}\right] \left[\begin{array}{c} \dfrac{\partial \hat{x}_\nu^{\ \beta}}{\partial a_p} \\ \hline \dfrac{\partial \hat{Z}_\alpha}{\partial a_p} \end{array}\right] = \left[\begin{array}{c} \dfrac{\partial^2 U}{\partial x_\mu^{\ \alpha} \partial a_p} \\ \hline 0 \end{array}\right] \tag{15}$$

where I denote a 3×3 identity matrix. The first order derivatives of $\hat{x}_\nu^{\ \beta}$ and $\hat{Z}_\alpha$ with respect to a_p form a $3N + 3$ by 6 matrix as do the constant terms on the right side of the equation. The second order derivatives of the energy function U with respect to the atomic coordinates form the upper left block of the 3N+3 by 3N+3 coefficient matrix Q and then can be denoted as

$$Q_{3(\mu-1)+\alpha, 3(\nu-1)+\beta} = \frac{\partial^2 U}{\partial x_\mu^{\ \alpha} \partial x_\nu^{\ \beta}}, \qquad \mu, \nu = 1, \cdots, N \quad \text{and} \quad \alpha, \beta = 1, \cdots, 3$$

Since the coefficient matrix Q is invertible, Eq.15 can be solved exclusively by multiplying both sides by Q^{-1}. The first order derivatives of $\hat{x}_\mu{}^\alpha(a_1, \cdots, a_6)$ with respect to a_p can therefore be calculated with the equations

$$\frac{\partial x_\mu{}^\alpha}{\partial a_p} = \sum_{\nu=1}^{N} \sum_{\beta=1}^{3} Q^{-1}_{3(\mu-1)+\alpha, 3(\nu-1)+\beta} \frac{\partial^2 U}{\partial x_\nu{}^\beta \partial a_p}. \tag{16}$$

Note that in Eq.16, only the upper left part of Q^{-1} was used as the summations are running from 1 to $3N$.

At the equilibrium configuration determined by Eq.2, the stress tensor components defined by Eq.7 can be calculated directly with functions $\hat{x}_\mu{}^\alpha(a_1, \cdots, a_6)$ from the first order derivatives of the energy function U with respect to the cell dimensions, as in the general regime

$$T^i = \frac{2}{V} \sum_{p=1}^{6} \frac{\partial a_p}{\partial g_i} (U_p + \sum_{\mu=1}^{N} \sum_{\alpha=1}^{3} \frac{\partial x_\mu{}^\alpha}{\partial a_p} \cdot \frac{\partial U}{\partial x_\mu{}^\alpha}) = \frac{2}{V} \sum_{p=1}^{6} \frac{\partial a_p}{\partial g_i} U_p \tag{18}$$

where for simplicity

$$U_p = \frac{\partial U(a_1, \cdots, a_6; x_\mu{}^\alpha)}{\partial a_p}. \qquad \mu = 1, \cdots, N \quad \text{and} \quad \alpha = 1, \cdots, 3$$

The combination of Eq.18 and Eq.2 then can be established as the equilibrium conditions for a crystal under zero as well as elevated pressures. Born and Huang (Born and Huang 1954) argued that with infinite lattice model, the equilibrium conditions for a crystal are that every atom of the crystal must be in equilibrium and that all stresses must also vanish inside the crystal. Indeed, as no deformation occurs at the stress free state, the stress calculated from Eq.18 must also equal zero for a crystal in addition to the requirements of Eq 2. This is the reason why the structure of a crystal under zero stress has to be determined by minimizing its energy function U with respect to both its cell dimensions and its atomic coordinates. For a crystal under stress, the atoms still have to be in their equilibrium

positions as required by Eq.2, since there are no net forces acting on them. The second condition, however, no longer holds as the tension or the stress induced from the initial deformation exists. Because infinite lattice model is being used here, the external forces can not be calculated explicitly in this study. Under the assumption of equilibrium, however, the external forces can still be calculated from Eq.18 by changing the sign of the resulting stress, as in reality, the induced stress must balance the externally applied forces near the surface of the crystal. Therefore, the determination of the structure of a crystal under stress corresponds to a constrained minimization problem with the minimization only being carried with respect to its internal atomic coordinates. Under hydrostatic pressure, the cell dimensions of the crystal can be determined by minimizing its energy function U at a constant volume. Then, in terms of the natural coordinate system, as the hydrostatic pressure can be written as

$$T^i = Pg^i$$

where P is the pressure specified in terms of the Cartesian coordinate systems and g^i is the element of G^{-1}, the reciprocal metrical tensor (International Table for X-ray Crystallography, Vol. 2), the applied pressure can be calculated with the equations

$$P = -\frac{2}{g^i V} \sum_{p=1}^{6} \frac{\partial a_p}{\partial g_i} U_p. \tag{19}$$

Also with functions $\hat{x}_\mu{}^\alpha(a_1, \cdots, a_6)$, the elastic constants of a crystal can be calculated directly in the general regime. By reindexing the atomic coordinates, $x_\mu{}^\alpha$, $\mu = 1, \cdots, N$ and $\alpha = 1, \cdots, 3$, with the energy expression

$$U = U(a_1, \cdots, a_6; x_1, \cdots, x_{3N}), \tag{20}$$

the second order derivatives of the energy function $\hat{U}$ with respect to the cell

dimensions in the macroscopic regime can be calculated as

$$\begin{aligned}\frac{\partial^2 \hat{U}}{\partial a_p \partial a_q} &= \frac{\partial^2 U}{\partial a_p \partial a_q} + \sum_{\alpha=1}^{3N} \frac{\partial \hat{x}_\alpha}{\partial a_p} \cdot \frac{\partial^2 U}{\partial x_\alpha \partial a_q} + \sum_{\beta=1}^{3N} \frac{\partial \hat{x}_\beta}{\partial a_q} \cdot \frac{\partial^2 U}{\partial x_\beta \partial a_p} \\ &\quad + \sum_{\alpha=1}^{3N} \sum_{\beta=1}^{3N} \frac{\partial \hat{x}_\alpha}{\partial a_p} \cdot \frac{\partial \hat{x}_\beta}{\partial a_q} \cdot \frac{\partial^2 U}{\partial x_\alpha \partial x_\beta} \\ &= U_{pq} + \sum_{\alpha=1}^{3N} \frac{\partial \hat{x}_\alpha}{\partial a_p} U_{\alpha q} + \sum_{\beta=1}^{3N} \frac{\partial \hat{x}_\beta}{\partial a_q} U_{\beta p} + \sum_{\alpha=1}^{3N} \sum_{\beta=1}^{3N} \frac{\partial \hat{x}_\alpha}{\partial a_p} \frac{\partial \hat{x}_\beta}{\partial a_q} U_{\alpha\beta}\end{aligned} \tag{21}$$

where

$$U_{pq} = \frac{\partial^2 U}{\partial a_p \partial a_q}, \quad U_{\alpha q} = \frac{\partial^2 U}{\partial x_\alpha \partial a_q} \quad \text{and} \quad U_{\alpha\beta} = \frac{\partial^2 U}{\partial x_\alpha \partial x_\beta}.$$

Substituting Eq.16 into Eq.21 then yield

$$\begin{aligned}\frac{\partial^2 \hat{U}}{\partial a_p \partial a_q} &= \frac{\partial^2 U}{\partial a_p \partial a_q} - \sum_{\alpha=1}^{3N} \sum_{\beta=1}^{3N} \frac{\partial^2 U}{\partial a_p \partial x_\alpha} (Q^{-1}_{\alpha\beta}) \frac{\partial^2 U}{\partial x_\beta \partial a_q} \\ &= U_{pq} - \sum_{\alpha=1}^{3N} \sum_{\beta=1}^{3N} U_{p\alpha} Q^{-1}_{\alpha\beta} U_{\beta q}\end{aligned} \tag{22}$$

with the fact derived from Eq.15

$$\sum_{\gamma=1}^{3N} \sum_{\lambda=1}^{3N} Q^{-1}_{\alpha\gamma} Q_{\gamma\lambda} Q^{-1}_{\lambda\beta} = Q^{-1}_{\alpha\beta}.$$

Finally from Eq.8, the elastic constants of the crystal can be calculated from the energy expression U with the equations

$$C^{ij} = \frac{4}{V} \Big\{ \sum_{p=1}^{6} \frac{\partial^2 a_p}{\partial g_i \partial g_j} U_p + \sum_{p=1}^{6} \sum_{q=1}^{6} \frac{\partial a_p}{\partial g_i} \cdot \frac{\partial a_q}{\partial g_j} (U_{pq} - \sum_{\alpha=1}^{3N} \sum_{\beta=1}^{3N} U_{p\alpha} Q^{-1}_{\alpha\beta} U_{\beta q}) \Big\} \tag{23}$$

where the terms involving the derivatives of the energy expression U only with respect to the cell dimensions are defined as the external elastic constants and the terms that involve the atomic coordinates are defined as the inner elastic constants.

Using Eq.23, the elastic constants of a crystal can be calculated with a potential of any form, as long as the energy per unit cell of the crystal can be expressed

as a function of the cell dimensions and the atomic coordinates. The derivatives of the energy function can also be evaluated analytically, although in our calculations, they were calculated numerically with the finite difference method (Abramowitz and Stegun pp-883). Before an elastic constant calculation can be made, however, one thing need be emphasized that the structure of the crystal be optimized first by finding the atomic positions associated with a minimum of the energy per unit cell. Although in some previous calculations, the cell dimensions were clamped at the experimental values (Miyamoto and Takeda 1984; Sanders 1984; Catti 1989), they are also better included as variables in the calculations and can be determined under either zero or elevated pressures as stated earlier. Under pressure, the Brugger elastic constants C^{ijkl} calculated with Eq.23 need be converted to the effective elastic constants as they are the ones that determined from experiments (Thurston 1965; Wallace 1967). In the remainder of this paper, as the effective elastic constants are used most widely, they will still be denoted as C_{ijkl} except otherwise specified. Finally, if the crystal was specified with respect to a Cartesian coordinate system $C = \{\mathbf{i}, \mathbf{j}, \mathbf{k}\}$, the elastic constants C^{ijkl} can be transformed to those at the Cartesian coordinate system with the equation

$$[C_{ijkl}]_C = a_{ip} a_{jq} a_{kr} a_{ls} [C^{pqrs}]_D \tag{24}$$

where a_{ij} is the element of the transformation matrix.

A comparison of the elastic constants of quartz and cristobalite calculated from different potentials

In this study, the QLM potential derived by Boisen and Gibbs (1993) was used to calculate the elastic constants for quartz and cristobalite. Three of the theoretical potentials derived with the covalent model by Lasaga and Gibbs (1987, 1988) were also used, which are denoted as the covalent, the Urey-Bradley and the

Morse potentials, respectively. These four potentials were reported to be capable of reproducing the zero pressure structures of quartz and cristobalite to within a few percent as well as the volume compressibility curve of quartz up to 2 Gpa. As the elastic constants provide us with information about the curvatures of the energy function for a crystal at its equilibrium configuration, a comparison of the elastic constants calculated using these potentials with the experimental results is a more stringent test for them. Hence, if these potentials give a reasonable description of the binding forces within the crystals, then general agreement can also be expected between the calculated and the observed elastic constants.

In the case of quartz, where there are three units of SiO_2 per unit cell, 33 parameters are required, assuming $P1$ symmetry, to define its structure, if none of the atoms is assumed to be fixed at the origin. A minimization of the energy with respect to 33 variables, however, would be time consuming and expensive, particularly when the energy function is difficult to evaluate. To circumvent this problem, space group symmetry $P3_12_11$ was assumed during minimizations. In previous calculations, maintaining of the observed space group during the minimization was found not to affect the result adversely. For example, using the SQLOO potential, a minimization of the quartz structure, assuming only $P1$ symmetry, generated a structure with $P3_12_11$ symmetry to within 0.001Å (Downs, 1992). A similar calculation completed for coesite also generated a structure with $C2/c$ symmetry to within 0.001Å (Boisen and Gibbs 1993). In the following calculations, after the structures had been determined with the observed space group symmetry, the symmetry constraints were then relaxed to $P1$ to calculate the first and the second order derivatives of the energy per unit cell with respect to the cell dimensions and the atomic coordinates. For all of structures generated in this study, as the first order derivatives were always zero, they correspond at least to some critical

points under $P1$ symmetry with the potentials used. Then to further determine the stability of these structures, the eigenvalues of the second order derivatives had also been calculated. Using some of the potentials, the resulting structures were found to only correspond to saddle points under $P1$ symmetry, as negative eigenvalues were found. Also, the stability of these structures were determined in this study by checking whether the calculated elastic constants are positive definite or not.

In calculating the second order derivatives, the step length was tested for different values between 10^{-2} to 10^{-6}, as care must be exercised in choosing the step length appropriately (neither too large nor too small). Depending on the types of functions used in the potentials, stable results were found to obtain usually for the step lengths over the range between 10^{-4} to 10^{-5} (Close to that recommended by Dennis and Schnabel, 1983). Over this range, the calculated elastic constants do not change significantly with the use of different step lengths. Another criteria used in this study to determine the proper step length is to make sure that the lengths of the steps generate elastic constants that satisfy the relations imposed by the symmetry of the crystal (Nye, 1957). In the case of the potentials derived with the quadratic functions, it was found that the satisfaction of the symmetry relations could obtained up to the fifth or the sixth decimal place. For the other types of potentials, however, the symmetry relations were usually violated in the third decimal place due to the anharmonic effects of the functions used in these potentials.

For a trigonal crystal like quartz, there are seven nonequivalent elastic constants, but only six are independent with the relation $C_{66} = \frac{1}{2}(C_{11} - C_{12})$. The results of the calculations made with the four theoretical potentials are compared in Table 1 with the data obtained experimentally by McSkimin et al. (1965). Also

listed in Table 1 are the bulk moduli of the crystal calculated from the four sets of elastic constants. By inverting the 6×6 matrix of the resulting elastic constants, the bulk modulus can be calculated with the equation

$$K = 1/\sum_{i=1}^{3}\sum_{j=1}^{3} s_{ij} \tag{26}$$

where the elements of the inverted matrix, s_{ij}, are called the elastic compliance constants (Nye, 1957). These values agree to within ~3% with those calculated by Lasaga and Gibbs (1987, 1988) and Boisen and Gibbs (1993). The difference can be ascribed to different methods used by them to calculate the bulk modulus. In particular for the QLM potential, the bulk modulus of quartz was calculated by fitting a Birch-Murnaghan equation to the calculated volume compressibility curve (Boisen and Gibbs 1993). Despite the fact that the Birch-Murnaghan equation was derived for cubic crystals, the bulk modulus calculated with this equation is in close agreement with that obtained from the elastic constants.

Compared with the observed data, both the QLM and the covalent potential yield similar and reasonable results for the elastic constants of quartz, except for C_{11}, C_{12} and C_{13}. The values calculated for C_{11} using both the QLM and the covalent potentials are ~30% larger while the values calculated for C_{12} are ~70% larger than observed. Also, as the values calculated for C_{13} have an opposite sign to that observed, both potentials give an unrealistic negative Poisson's ratio for quartz along its c cell edge. The overall agreement of these results, however, is surprisingly good, considering that the potentials used in the calculations were derived entirely from the quantum mechanical calculations completed on the small molecules like $H_6Si_2O_7$. On the other hand, although the Urey-Bradley and the Morse potentials reproduce the bulk modulus of quartz, the agreement between the calculated and the observed elastic constants is less satisfactory. Not only are

Table 1. A comparison of the elastic constants (10^{11} dyn/cm^2) and bulk modulus (GPa) of quartz calculated from the four theoretical potentials (Boisen and Gibbs 1993; Lasaga and Gibbs 1987, 1988) with the experimental results (McSkimin et al. 1965).

	QLM	Covalent	Urey-Bradley	Morse	Experiment
C_{11}	12.76	13.17	6.20	5.40	8.76
C_{12}	3.53	2.64	3.21	2.13	.99
C_{13}	-1.12	-.75	3.00	1.83	1.30
C_{14}	-1.77	-2.59	-.37	-.53	-1.77
C_{33}	11.51	9.79	5.31	4.48	10.92
C_{44}	8.18	5.84	1.93	2.10	5.97
C_{66}	4.61	5.26	1.50	1.63	3.86
K	42.27	40.00	39.80	29.48	38.93

Table 2. A comparison of the calculated elastic constants (10^{11} dyn/cm^2) and bulk modulus (GPa) of cristobalite with the observed data (Yeganeh-Haeri et al. 1992). The potentials used in the calculations are the same as those in Table 1. The stars denote the unstable structures.

	QLM	Covalent	Urey-Bradley*	Morse*	Experiment
C_{11}	7.69	7.33	1.75	-4.22	5.94
C_{12}	7.69	7.33	4.81	9.96	.38
C_{13}	-2.16	-1.95	1.13	0.58	-.44
C_{33}	6.95	5.58	2.57	2.35	4.24
C_{44}	8.16	8.24	2.20	2.50	6.72
C_{66}	5.67	5.19	1.04	1.20	2.57
K	25.69	22.06	19.94	15.84	16.00

the values calculated for C_{11} and C_{33} only half those observed, but also the values calculated for the shear elastic constants C_{44} and C_{66} are very small. In light of this result, the $P3_12_11$ structures generated with the Urey-Bradley and the Morse potentials were found to be only metastable under $P1$ symmetry.

Using the same potentials, similar calculations were completed for cristobalite, assuming $P4_12_12$ symmetry and four units of SiO_2 per unit cell. The values calculated for the six nonequivalent elastic constants of cristobalite are compared in Table 2 with the results obtained in a Brillouin spectroscopic study (Yeganeh-Haeri et al. 1992). Calculated from the Urey-Bradley and the Morse potentials, the structures of cristobalite were found to be unstable under $P1$ symmetry with no meaningful elastic constants. Also using the QLM and the covalent potentials, the agreements of the calculated elastic constants with the observed data were found not as good as those for quartz. As the bulk moduli calculated with both sets of elastic constants are larger than observed, both the QLM and the covalent potentials predict that cristobalite is stiffer than expected. This may be ascribed, however, to the fact that the SiOSi angle in cristobalite (146.4°) is wider than that in quartz (142.3°). As a wider angle is, in general, associated with a weaker bond, one may expect that the force constant associated with the SiOSi angle in cristobalite is overestimated by both the QLM and the covalent potentials, which were derived from the force field of $H_6Si_2O_7$ with narrower SiOSi angles that are 137° and 144°, respectively. The argument is also supported by the fact that the elastic constants of cristobalite calculated from both the QLM and the covalent potential overestimate the experimental results systematically. In particular, as the QLM potential was derived with a much narrower SiOSi angle, it predicts a larger bulk modulus for cristobalite than the covalent potential does. Thus, if the results of the calculations were scaled properly, reasonable agreement between

the calculations and the experimental results can still obtain except for C_{12}, for which the calculated values are too large and lead the structures determined under $P4_12_12$ symmetry constraint almost unstable under $P1$ symmetry. The negative values calculated for C_{13} are also consistent with the observation that the Poisson's ratio of cristobalite is negative (Yeganeh-Haeri et al. 1992).

For quartz and cristobalite, calculations of the elastic constants were also completed in this study using three semi-empirical potentials, which include the SQLOO potential derived with the covalent model by Boisen and Gibbs (1993) and two potentials derived with the ionic model by Tsuneyuki et al. (1988) and van Beest et al. (1993), respectively. For the ionic potentials, the Ewald's method was used to accelerate the convergence of the electrostatic interactions. The results of the calculations are listed in Table 3 and Table 4 for quartz and cristobalite, respectively. Among these calculations, the elastic constants of quartz calculated from the ionic potentials agree closely with the calculations made by van Beest et al. (1991) and Purton et al. (1993). Using the SQLOO potential, as two minima result for quartz with slightly different energy (Boisen and Gibbs 1993), two set of elastic constants were calculated for quartz with those calculated at the structure of higher energy agreeing slightly better with the observed values. The opposite sign with respect to the values calculated for C_{14} is due to the fact that by maintaining $P3_12_11$ symmetry during the minimizations, these two structures were found to be related approximately by a half turn along the c cell edge such as that observed between Dauphiné twins. Since quartz lacks the half turn symmetry along its c cell edge, a rotation like this by 180° changes its elastic constant C_{14} from being positive to being negative or vice versa. Also with a mirror plane, the change of its structure from that of the left hand one to that of the right hand one has the same effect for quartz. Thus for a trigonal crystal like quartz, its elastic

Table 3. A comparison of the elastic constants (10^{11} dyne/cm^2) and the bulk modulus (GPa) of quartz calculated from the three semi-empirical potentials (Boisen and Gibbs 1993; van Beest et al. 1991; Tsuneyuki et al. 1988) with the experimental results (McSkimin et al. 1965).

	Boisen and Gibbs		van Beest	Tsuneyuki	Experiment
C_{11}	10.08	9.96	9.01	7.15	8.76
C_{12}	2.96	2.93	.90	.96	.99
C_{13}	.28	.28	1.59	1.24	1.30
C_{14}	1.24	-1.23	-1.74	-1.40	-1.77
C_{33}	9.16	9.25	10.89	9.30	10.92
C_{44}	5.41	5.42	5.05	4.05	5.97
C_{66}	3.56	3.51	4.06	3.10	3.87
K	39.44	39.36	40.64	33.26	38.93

Table 4. A comparison of the calculated elastic constants (10^{11} dyne/cm^2), bulk modulus (GPa) and Poisson's ratio of cristobalite with the observed data (Yeganeh- Haeri et al. 1992). The potentials used in the calculations are the same as those in Table 3. The star denotes the unstable structure.

	Boisen and Gibbs*	van Beest	Tsuneyuki	Experiment
C_{11}	5.40	6.76	5.14	5.94
C_{12}	6.29	1.02	.78	.38
C_{13}	-1.19	.11	-.09	-.44
C_{33}	4.66	4.42	3.66	4.24
C_{44}	5.69	7.18	5.87	6.72
C_{66}	3.88	2.51	1.87	2.57
K	20.03	21.22	15.91	16.00
σ	-.10	.01	-.02	-.07

constant C_{14} can be either positive or negative, depending on the arrangement of the atoms. This is also consistent with the previous experimental results for quartz, where both positive and negative values have been reported for C_{14} as shown from the data compiled by Ohno (1991).

Also based on a covalent model and determined from a force field calculated for the molecule $H_6Si_2O_7$, the SQLOO potential modifies the QLM and the covalent potentials with a repulsion term for the non-codimer oxygen atoms being incorporated. The force constants associated with the SiO bonds are also scaled proportionally. Empirically, the scaling constant and the repulsion term in the SQLOO potential were determined to reproduce the volume compressibility curve of quartz up to 8 GPa (Boisen and Gibbs 1993). Using the SQLOO potential, the agreement of the calculated elastic constants with the experimental data was also found being improved significantly. In particular, using the same potential, the value calculated for C_{13} of quartz is positive while that obtained for cristobalite is negative and yields a negative Poisson's ratio along its c cell edge. Several unsatisfactory features, however, still need be pointed out. For quartz, the value calculated for C_{11} using the SQLOO model potential is still higher than that calculated for C_{33}, although their agreement with the observed data is improved from those calculated using the QLM and the covalent potentials. Contrary to the experimental observations, these calculations predict that under pressure, the c cell edge of quartz decreases faster than its a cell edge. Also, the calculated C_{12} is too large and the calculated C_{13} is too small. For cristobalite, the calculated C_{12} is extremely large. This is a more serious problem, as it results that the elastic constants calculated for cristobalite with the SQLOO potential are not positive definite.

Compared with the calculations made using the SQLOO potential, the ionic

potentials derived by van Beest et al. (1991) and by Tsuneyuki et al. (1988) give results that are in better agreement with the experimental values. Although it was derived from the theoretical calculation, the van Beest et al. (1991) potential was also derived by parameterizing the potential energy function until the calculated elastic constants match those observed for quartz to within several percent. On the other hand, as the Tsuneyuki et al. (1988) potential was derived, in addition to the theoretical calculation, with only the compressibility data for quartz measured by Levien et al. (1982), the elastic constants calculation using the resulting potential yields a set of elastic constants and bulk modulus (33.3GPa) for quartz that are slightly smaller than those observed. Calculations of the elastic constants and the bulk modulus for cristobalite using the two ionic potentials also resulted in values that are in good agreement with the data obtained by Yeganeh-Haeri et al. (1992). Despite of this good agreement, both potentials failed to reproduce the negative Poisson's ratio correctly for the mineral. Using the van Beest et al. (1991) potential, a positive Poisson's ratio was calculated for cristobalite along its c cell edge with the C_{13} being positive while the Tsuneyuki et al. (1988) potential yields a negative value for C_{13} that it is very close to zero (-0.091). Calculated from the three sets of the resulting elastic constants, the Poisson's ratios of cristobalite along its c cell edge are also given in Table 4. Compared with that calculated from the experimental data (Yeganeh-Haeri et al. 1992), the SQLOO potential gives the best agreement. The value calculated with the SQLOO potential in this study also agrees closely with that calculated previously by Boisen and Gibbs (1993).

In a further examination of the semi-empirical potentials, pressure derivatives of the elastic constants calculated for quartz are compared in Table 5 with the experimental values (McSkimin et al. 1965). The equilibrium structures of quartz at elevated pressures were determined by minimizing its energy per unit cell as-

Table 5. A comparison of the pressure derivatives of the elastic constants of quartz calculated from the semi-empirical potentials used in Table 3 with the experimental results (McSkimin et al. 1965).

	Boisen and Gibbs	van Beest	Tsuneyuki	Experiment
C'_{11}	1.67	1.71	2.73	3.40
C'_{12}	3.50	6.98	6.79	7.40
C'_{13}	4.05	6.40	6.75	5.41
C'_{14}	1.19	2.16	2.76	2.00
C'_{33}	7.83	14.75	15.96	10.26
C'_{44}	.93	1.21	1.16	1.77
C'_{66}	-.91	-2.64	-2.03	-2.00
K'	4.16	5.79	6.18	5.8

suming both $P3_12_12$ symmetry and constant volumes. At the structure minimized at a constant volumes, the stress calculated was found to agree with hydrostatic pressure out to the fifth decimal place. The derivatives of the elastic constants were calculated by fitting the effective elastic constants at different pressures with a straight line up to $\sim$1 GPa. Although the elastic constants of a crystal do not, in general, vary linearly with pressure, the linear interpolation was found in our calculations to be a reasonable approximation for quartz up to $\sim$1 GPa as observed by McSkimin et al. (1965) that it is within the error of experiment.

As the SQLOO pressure derivatives of the elastic constants underestimate the experimental result, quartz is predicted to be softer than observed. Nonetheless, the signs of the derivatives generated in the three semi-empirical potentials are correct. The overall agreement between the observed and calculated data sets is also very good, particularly when compared with the calculation made with the ionic shell model potential by Purton et al. (1993). In their calculation, although the pressure derivatives of the elastic constants of quartz have not been reported, they found, contrary to the experimental result, that most of the diagonal elastic constants decrease with the increase of pressure. Also, they reported that the value calculated for C_{33} increases at a slower rate than observed. Thus, a calculation using the ionic shell model potential should yield a pressure derivative of the bulk modulus that is much smaller than that observed. On the other hand, both the SQLOO potential and the ionic potentials reproduce the pressure derivative of the bulk modulus for quartz. For the two ionic potentials, as the pressure derivative of C_{33} is overestimated, they yield pressure derivatives of the bulk modulus that are in better agreement with that observed than that calculated from the SQLOO potential.

Recently, simulated annealing strategies have been used with the SQLOO po-

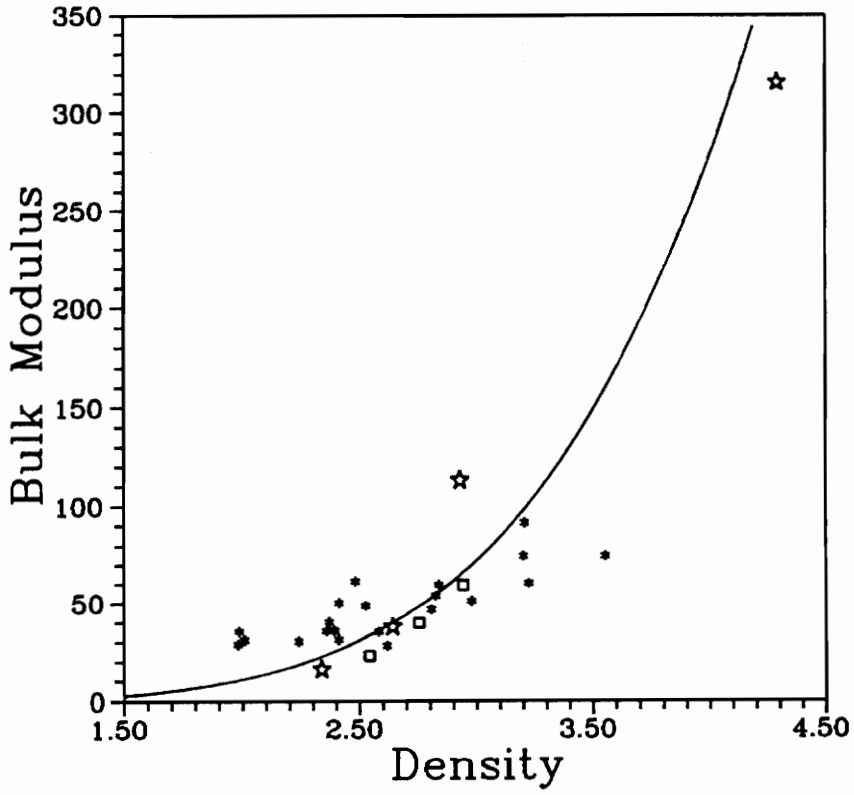

Fig. 1. Bulk modulus versus density for the hypothetical structures generated by the SQLOO potential. The stars denote the experimental data for cristobalite, quartz, coesite and stishovite. The diamonds denote the calculated data with the SQLOO potential for these crystals. The asterisks denote the data calculated using the SQLOO potential for the other hypothetical structures.

tential to generate 23 distinct framework structures for silicas (Boisen and Gibbs, to be published). For these hypothetical structures, elastic constant calculations were completed to test an empirical relation between the bulk modulus and the density proposed for oxides (Anderson and Nafe 1965). The aggregate bulk modulus was obtained in this study by computing the Voigt and the Ruess bounds of the calculated elastic constants. The resulting bulk moduli are then plotted in Fig. 1 against the density for these hypothetical structures. The curve in the figure was calculated from the experimental data obtained for quartz (McSkimin et al. 1965), cristobalite (Yeganeh-Haeri et al. 1992), coesite (Weidner and Car-

leton 1977) and stishovite (Weidner et al. 1982). From the experimental data, the bulk modulus of silica polymorphs can be related to the density with the equation $K = C \times \rho^{-4.6}$, a curve that is close to the empirical relation $K = C \times \rho^{-4.0}$ proposed for oxides. Calculated using the SQLOO potential, Fig. 1 shows that the bulk moduli of the hypothetical structures also increase with the density roughly at the same trend provided by the experimental data, although for the structures of high density, the bulk modulus tends to underestimate the value predicted from the empirical relation.

Calculation of the elastic constants of quartz and cristobalite as functions of pressure

Because the three semi-empirical potentials used in this study are capable of reproducing the pressure derivatives of elastic constants of quartz reasonably well, elastic constant calculations were completed for quartz and cristobalite as functions of pressure up to their transitional pressures. As the elastic constants of minerals at high pressures are essential for the interpretations of the seismic wave velocity profiles, a knowledge of such data is important in geophysics. Because of difficulties in experiments, the elastic constants at high pressure have yet to be measured. So to compensate for the lack of such data, theoretical calculations would be useful, particularly if they can provide reasonable estimates of the true values. By calculating the elastic constants of quartz at the high pressures, insight can also be gained into the mechanisms involved in its pressure induced amorphous transition. From the molecular dynamical calculations completed under pressure using the potentials derived by van Beest et al. (1992) and Tsuneyuki et al. (1988), Tse and Klug (1991), Binggeli and Chelikowsky (1992) and Chaplot and Sikka (1993) found that the quartz structure becomes unstable above ~22 GPa. As this pressure is consistent with the observation that quartz transforms gradually to an

amorphous form at pressure above 25 GPa, they concluded that the driving force behind the amorphization of quartz is the mechanical instability of the quartz structure under high pressure.

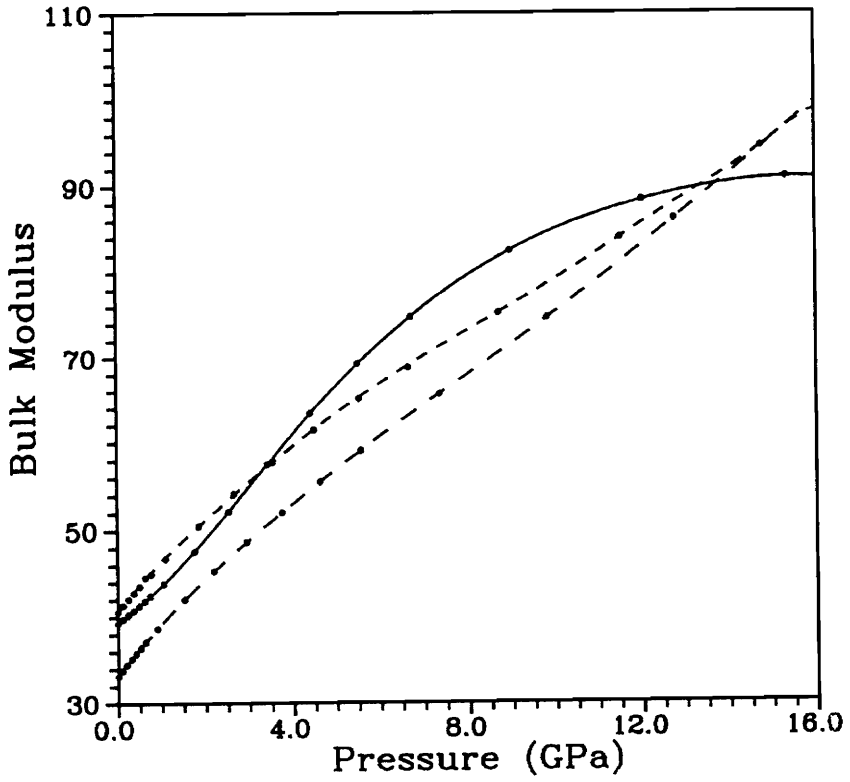

Fig. 2. Bulk modulus versus pressure for quartz. The solid line denotes the calculation made with the SQLOO potential (Boisen and Gibbs 1993). The short dashed line denotes the calculation made with the van Beest et al. (1990) potential. The longer dashed line denotes the calculation made with the Tsuneyuki et al. (1988) potential.

From the elastic constants calculated at elevated pressures, the bulk modulus was also calculated for quartz and cristobalite as a function of pressure. The bulk modulus of quartz calculated using the three semi-empirical potentials is plotted in Fig. 2 against pressure up to 16 GPa. Among the three curves obtained in the calculations, the one calculated with the SQLOO potential is exactly the same as that obtained by Boisen and Gibbs (1993). Using both of the ionic potentials,

the values calculated for the bulk modulus were found to increase almost linearly with pressure. On the other hand, the calculation made with the SQLOO potential predicts a nonlinear behavior of the bulk modulus. Although at pressures below 5 GPa, the bulk modulus calculated with the SQLOO potential increases roughly at the same rate as those calculated with the ionic potentials, it increases at a slower rate as the pressure increases. In particular, at pressures above ~12 GPa, the SQLOO potential generated a bulk modulus that does not change much with increasing pressure.

The behavior of the bulk modulus can be explained in terms of the variations of the elastic constants calculated as functions of pressure. Fig. 3 shows that using the two ionic potentials, most of the elastic constants of quartz also vary approximately linearly with pressure except for C_{44} and C_{66}. Using the SQLOO potential, however, most of the calculated elastic constants vary nonlinearly with increasing pressure. In particular, it is noteworthy that using the SQLOO potential, the value calculated for C_{11} increases with pressure until ~8 GPa and then begins to decrease. Although the value calculated for C_{33} increases rapidly at high pressures, the combination of C_{11} and C_{33} yields a nearly constant bulk modulus for quartz. As the value calculated for C_{12} increases steadily with pressure, the decrease of C_{11} is important and indicates that the structure of quartz is unstable at pressures above ~23 GPa, where $C_{11} - C_{12}$ falls below zero. The unstable structure is also indicated by the fact that C_{66}, which is related to C_{11} and C_{12} with the equation $C_{66} = \frac{1}{2}(C_{11} - C_{12})$, is decreasing. Thus, using the SQLOO potential, the amorphous transition of quartz can also be explained. For the ionic potentials, as the values calculated for C_{66} increase with pressure above ~5 GPa, the unstable structure of quartz results from the increasing of C_{14} and the decreasing of C_{44} as calculated by Binggeli and Chelikowsky (1992).

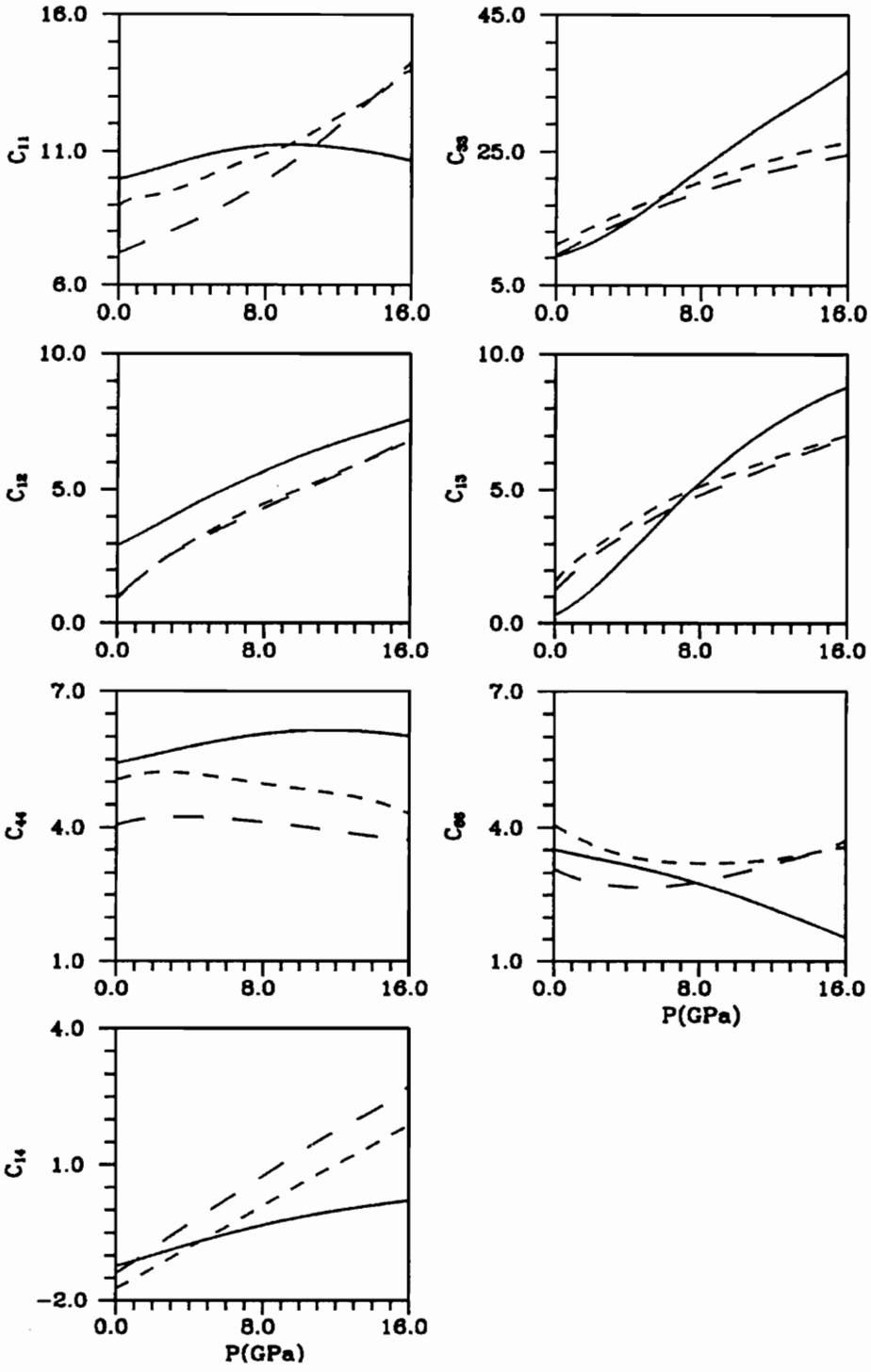

Fig. 3. Elastic constants versus pressure for quartz up to 16 GPa. The symbols are the same as in Fig. 2.

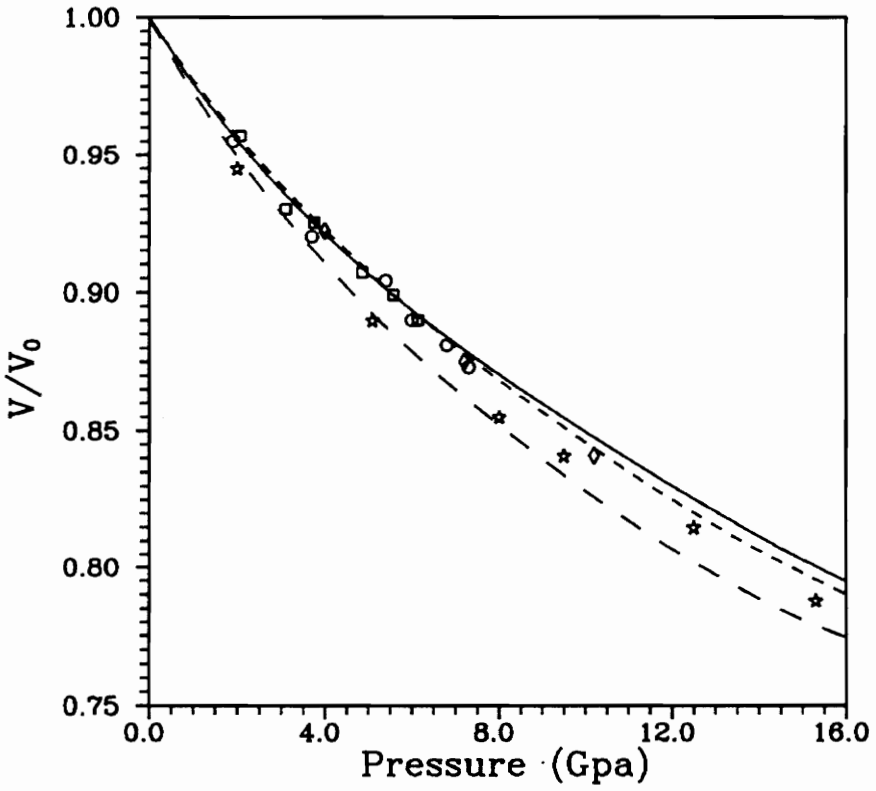

Fig. 4. Volume compressibility curves of quartz generated by the SQLOO potential (solid line), the van Beest et al. potential (short dashed line) and the Tsuneyuki et al. potential (longer dashed line) together with the experimental data. The stars denotes the Hazen et al. (1989) data. The diamonds denote the Glinnemann et al. (1992) data. The squares denote Levien et al. (1980) data. The circles denote the D'Amour et al. (1979) data.

Because of the paucity of the elastic constant data determined as functions of pressure, comparisons were made only between the calculated compressibility data and those measured in X-ray diffraction studies. For quartz, the volume compressibility curves calculated with the three potentials are drawn in Fig. 4 together with the observed data points (D'Amour et al. 1979; Levien et al. 1980; Hazen et al 1989; Glinnemann et al. 1992). As the Tsuneyuki et al. (1988) potential yields a smaller bulk modulus for quartz at zero pressure, the calculated volume compressibility curve underestimates the experimental data systematically. On the other hand, the van Beest et al. (1991) and the SQLOO potentials generate

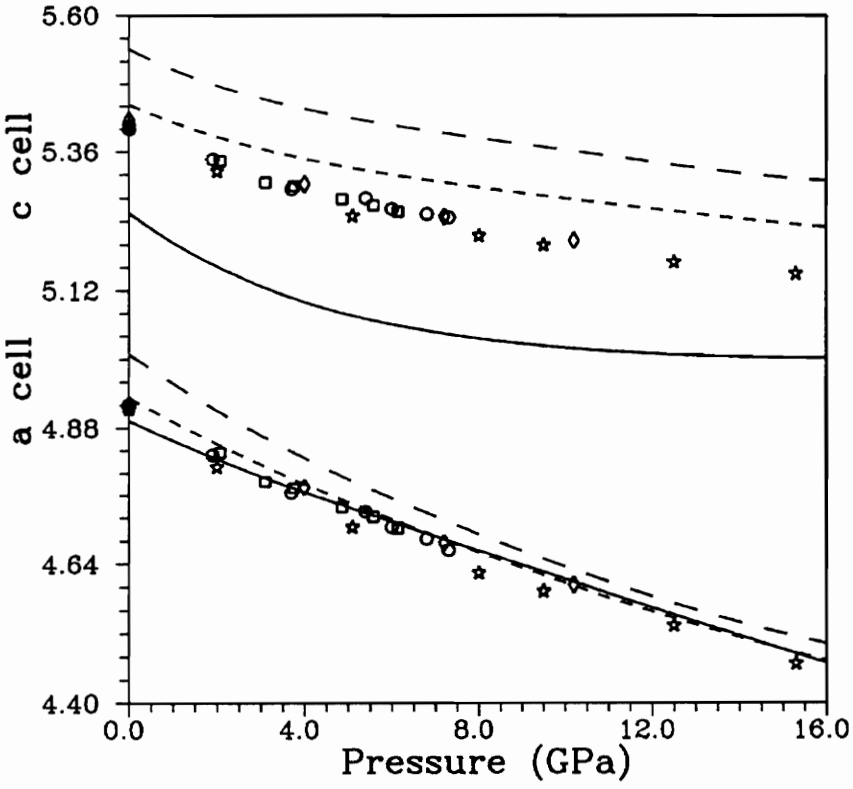

Fig. 5. The variations of the cell edges of quartz with pressure together with the experimental data. The symbols are the same as in Fig. 4.

compressibility curves that match the observed data up to ~16GPa. In Fig. 5, the compression of the cell edges is plotted against pressure for quartz. As revealed by the elastic constants C_{11} and C_{33} calculated at zero pressure, the SQLOO potential does not reproduce cell edge variations with increasing pressure as well as do the ionic potentials at low pressure. The SQLOO calculations completed at high pressure, however, yield cell dimension data that agree more closely with experimental data, as at pressures above 10 GPa, the calculations indicate that both the a cell and the c cell edges of quartz decrease with pressure at rates that agree roughly with those determined by Hazen et al. (1989) data.

From the X-ray diffraction studies, cristobalite was found to be very soft in that its volume decreases rapidly with increasing pressure. Using the SQLOO

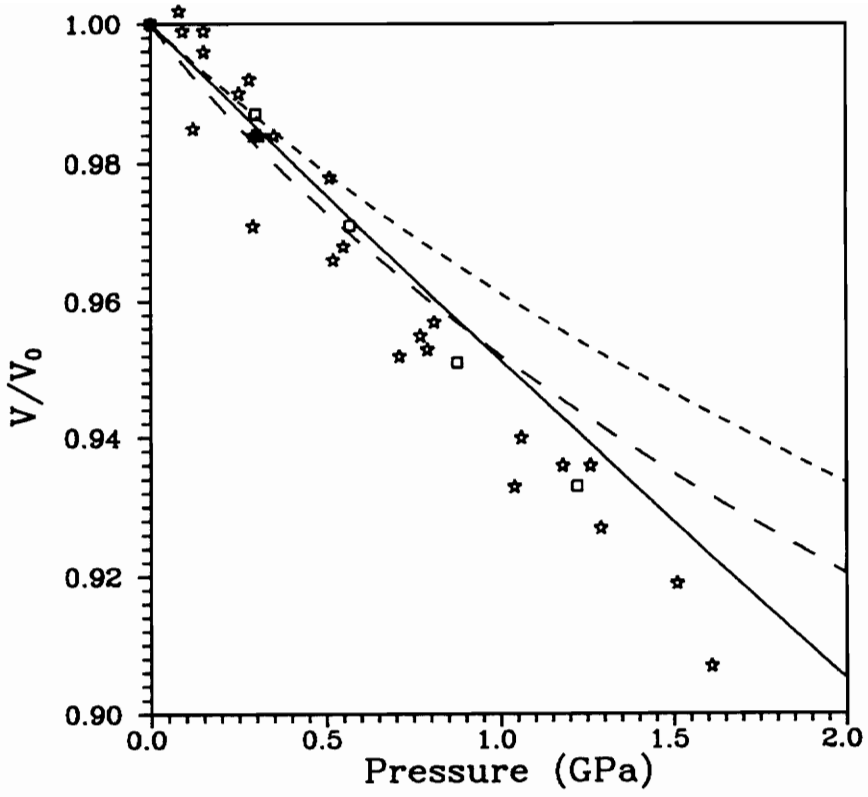

Fig. 6. Volume compressibility curves of cristobalite generated by the SQLOO potential (solid line), the van Beest et al. potential (short dashed line) and the Tsuneyuki et al. potential (longer dashed line) together with the experimental data. The stars denote the Downs and Palmer (1994) data. The squares denote the Yeganah-Haeri et al. (pensonal communication) data.

potential, the calculated elastic constants and the bulk modulus of cristobalite were found to be almost invariant with respect to increasing pressure. On the other hand, both of the ionic potentials indicate that the elastic constants and the bulk modulus of cristobalite increase rather dramatically. To compared with the experimental data (Yeganeh-Haeri et al. personal communication; Downs and Palmer 1994), the calculated volume compressibility curves of cristobalite and the compression of its cell edges are plotted in Fig. 6 and Fig. 7, respectively. The curves generated from the SQLOO potential roughly parallel the experimental data whereas the curves generated with the other two potentials depart from the

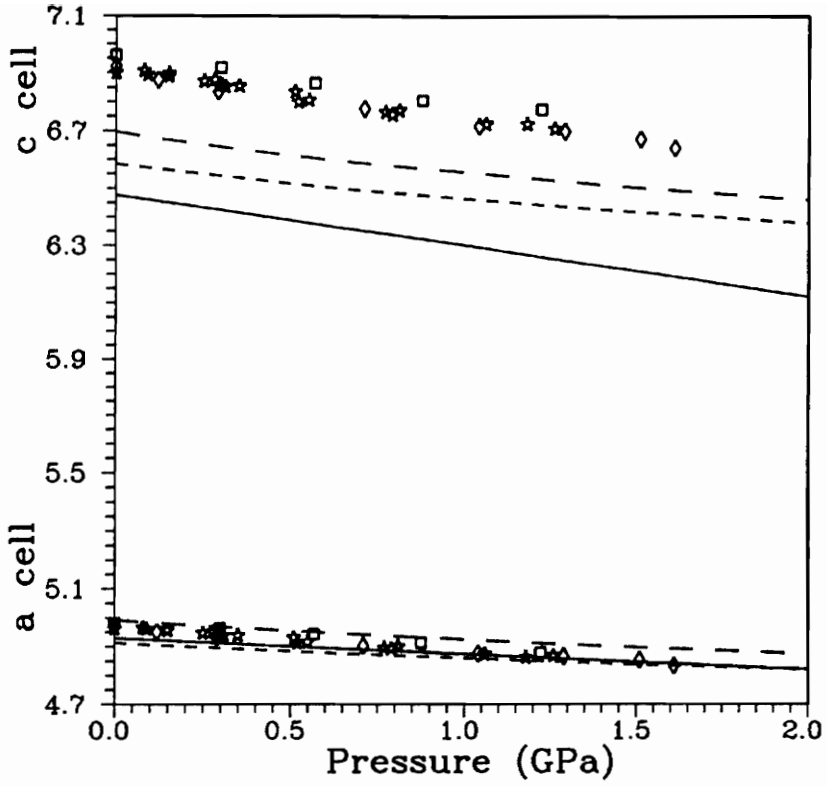

Fig. 7. The variations of the cell edges of cristobalite with pressure together with the experimental data. The symbols are the same as in Fig. 6.

data at pressures in excess of ~1 GPa. Consequently, as the structural behaviors of cristobalite are better modeled by the SQLOO potential under pressure, it is more reasonable that the elastic constants and bulk modulus of cristobalite are invariant with respect to increasing pressure.

Conclusion

Assuming homogeneous deformations, a method has been devised in this study to calculate the elastic constants of crystals both at zero pressure and as functions of pressure. Because this method can be applied to crystals of any symmetry using a wide range of potentials, these potentials can be tested by comparing the theoretical calculations with the experimental results. Using the three semi-empirical potentials, the elastic constants calculated for quartz and cristobalite at zero pres-

sure match the observed data. Consequently, combined with the compressibility data, the elastic properties of these crystals calculated at high pressure may serve to extend the experimental results to the high pressures.

Using potentials derived from *ab initio* energy surfaces calculated for simple molecules, elastic constants have been calculated for both quartz and cristobalite. Among the four theoretical potentials, two potentials derived with SiO bond lengths, OSiO and SiOSi bond angles as variables yield reasonable agreement with experimental data. As these potentials had been derived entirely from *ab initio* calculation, the calculations support the assertion that the binding forces in crystal are similar to those in the small molecules (Gibbs 1982). Also, as these two potentials yield better result than the other two, which were derived with the pairwise functions involving the SiO, SiSi and OO interaction, it may be concluded that the binding forces in these crystals are better described by the force fields associated with the bond streching and angle bending terms.

The semi-empirical potentials derive by Boisen and Gibbs (1993), van Beest et al. (1991) and Tsuneyuki et al. (1988) have also been used to calculate the elastic constants of quartz and as functions of pressure. Calculations completed using the ionic potentials yields elastic constants that vary almost linearly with pressure whereas those calculated with a covalent potential (SQLOO) were found to vary nonlinearly with increasing pressure in the region of the amorphous transition pressure. At zero pressure, although the SQLOO potentials yields slightly worse results, all of the three potentials are capable of reproducing the existing experimental data to certain extent. Also using the SQLOO potential, the agreement of the calculations with the experimental data has been improved substantially, compared with the calculations made using the theoretical potentials. As the SQLOO potential was mainly derived from a local force field, the good

agreements between the calculations made using the SQLOO potential and the experimental data suggest that it may not be necessary to include the strong Couloumbic force in a model in order for it to be effective in modeling the elastic properties of quartz even under high pressures.

Although its calculated elastic constants using the ionic potentials are in better agreement with the observed data, several interesting features of cristobalite have not been reproduced, including its negative Poisson's ratio and its softness under pressure. Using both of the two ionic potentials, the calculated elastic constants and bulk modulus of cristobalite were found to increase rapidly with increasing pressure. On the other hand, those generated from the SQLOO potential are almost invariant with their pressure derivatives being close to zero. As the structures of cristobalite are better modeled under pressure by the SQLOO potential, the nearly constants bulk modulus seems to be in better agreement with the X-ray diffraction studies.

References

Abramowitz, M. and Stegun, I.A. (1965) Handbook of mathematical functions with formulas graphs and mathematical tables. 1045 pp, Dover publications, Inc.: New York.

Anderson, O.L. and Nafe, J.E. (1965) The bulk modulus-volume relationship for oxide compounds and related geophysical problems. Journal of Geophysical Research, 70: 3951-3963.

Barron, T.H.K., Gibbons, T.G. and Munn, R.W. (1971) Thermodynamics of internal strain in perfect crystals. Journal of Physics, C: Solid State Physics, 4: 2805-2821.

Barron, T.H.K. and Klein, M.L. (1965) Second-order elastic constants of a solid under stress. Proceeding of Physical Sociaty, 85: 523-531.

Binggeli, N. and Chelikowsky, J.R. (1992) Elastic instability in α-quartz under pressure. Physical Review Letters, 69: 2220-2223.

Boisen, Jr., M.B. and Gibbs, G.V. (1993) A modeling of the structure and compressibility of quartz with a molecular potential and its transferability to cristobalite and coesite. Physics and Chemistry of Minerals, 20: 123-135.

Born, M. and Huang, K. (1954) Dynamical theory of crystal lattices. 420 pp, Clarendon press: Oxford.

Catlow, C.R.A. and Mackrodt, W.C. (1982) Computer simulation of Solid. Lecture notes in physics, 166: Chapter 1.

Catlow, C.R.A. and Price, G.D. (1990) Computer modeling of solid-state inorganic materials. Nature, 347: 243-248.

Catti, M. (1985) Calculation of elastic constants by the method of crystal static deformation. Acta Crystallographica, A41: 494-500.

Catti, M. (1989a) Crystal elasticity and inner strain: a computational model. Acta Crystallographica, A45: 20-25.

Catti, M. (1989b) Modeling of the structural and elastic changes of forsterite (Mg_2SiO_4) under stress. Physics and Chemistry of Minerals, 16: 582-590.

Chaplot, S.L. and Sikka, S.K. (1993) Molecular-dynamics simulations of pressure-induced crystalline-to-amorphous transition in some corner-linked polyhedral compounds. Physical Review B, 47: 5710-5714.

Cousins, C.S.G. (1978) Inner elasticity. Journal of Physics, C: Solid State Physics, 11: 4867-4879.

D'Amour, H., Denner, W. and Schulz, H. (1979) Structure determination of α-quartz up to 68×10^8 Pa. Acta Crystallographica, B35: 550-556.

Dennis, Jr., J.E. and Schnabel, R.B. (1983) Numerical Methods for Unconstrained

Optimization and Nonlinear Equations. 378 pp, Prentice-Hall Inc: Englewood Cliffs, New Jersey.

Downs, R.D. (1992) Librational displacements of silicate tetrahedra in response to temperature and pressure. PhD Dissertation, Virginia Polytechnic Institute and State University: pp. 76. Blacksburg Virginia

Downs, R.D. and Palmer, D.C (1994) The Pressure Behavior of α-Cristobalite. American Mineralogist, 79: 9-14.

Gibbs, G.V. (1982) Molecules as models for bonding in silicates. American Mineralogist, 67: 421-450.

Glinnemann, J., King, Jr., H.E., Schulz, H., Hahn, T., LaPlaca, S.J. and Dacol, F. (1992) Crystal structures of the low-temperature quartz-type phases of SiO_2 and GeO_2 at elevated pressure. Zeitschrift für Kristallographie, 198: 177-212.

Hazen, R. M., Finger, L.W., Hemley, R.J. and Mao, H.K. (1989) High-pressure crystal chemistry and amorphization of α-quartz. Solid State Communications, 72: 507-511.

Lasaga, A.C. and Gibbs, G.V. (1987) Application of quantum mechanical potential surfaces to mineral physics calculations. Physics and Chemistry of Minerals, 14: 107-117.

Lasaga, A.C. and Gibbs, G.V. (1988) Quantum mechanical potential surfaces and calculations on minerals and molecular clusters I STO-3G and 6-31G* results. Physics and Chemistry of Minerals, 16: 29-41.

Levien, L., Prewitt, C.T. and Weidner, D.J. (1980) Structure and elastic properties of quartz at pressure. American Mineralogist, 65: 920-930.

Miyamoto, M.T. and Takeda, H. (1984) An attempt to simulate high pressure structures of Mg-silicates by an energy minimization methods. American Mineralogist, 69: 711-718.

McSkimin, H.J., Andreatch, Jr., P. and Thurston, R.N. (1965) Elastic moduli of quartz versus hydrostatic pressure at 25° and -195.8° C. The Journal of Applied Physics, 36: 1624-1632.

Nye, J.F. (1957) Physical properties of crystals; their representation by tensors and matrices. 329 pp, Clarendon Press: Oxford.

Ohno, I. (1990) Rectangular parallellepiped resonance method for piezoelectric crystals and elastic constants of α-quartz. Physics and Chemistry of Minerals, 17: 371-378.

Price, G.D. and Parker, S.C. (1984) Computer simulations of the structural and physical properties of the olivine and spinel polymorphs of Mg_2SiO_4. Physics and Chemistry of Minerals, 10: 209-216.

Protter, M.H. and Morrey, C.B. (1977) A first course in real analysis. 507 pp, Springer-Verlag: New York Inc.

Purton, J., Jones, R., Catlow, C.R.A. and Leslie, M. (1993) Ab initio potentials for the calculation of the dynamical and elastic properties of α-quartz. Physics and Chemistry of Minerals, 19: 392-400.

Sanders, M.J., Leslie, M. and Catlow, C.R.A. (1984) Interatomic potentials for SiO_2. The Journal of the Chemical Society, Chemical Communications, 19: 1271-1273.

Toupin, R.A. and Bernstein, B. (1961) Sound waves in deformed perfectly elastic materials. Acoustoelastic effect. The Journal of the Acoustical Society of America, 33: 216-225.

Tse, J.S. and Klug, D. (1991) Mechanical instability of α-quartz: a molecular-dynamics study. Physical Review Letters, 67: 3559-3562.

Tsuneyuki, S., Tsukada, M., Aoki, H. and Matsui, Y. (1988) First-principles interatomic potential of silica applied to molecular dynamics. Physical Review Letters, 61: 869-872.

van Beest, B.W.H., Kramer, G.J. and van Santen, R.A. (1990) Force fields for silicas and aluminophosphates based on *ab initio* calculations. Physical Review Letters, 64: 1955-1958.

Yeganeh-Haeri, A., Weidner, D.J. and Parise, J.B. (1992) Elasticity of α-cristobalite: a silicon dioxide with a negative poisson's ratio. Science, 257: 650-652.

Wall, A., Parker, S.C. and Watson, G.W. (1993) The extrapolation of elastic moduli to high pressure and temperature. Physics and Chemistry of Minerals, 20: 69-75.

Wallce, D.C. (1965) Lattice dynamics and elasticity of stressed crystals. The Reviews of Modern Physics, 37: 57-67.

Wallce, D.C. (1967) Thermoelasticity of stressed materials and comparison of various elastic constants. Physical Review, 162: 776-789.

Weidner, D.J. and Carleton, H.R. (1977) Elasticity of coesite. JGR, 82: 1334-1346.

Weidner, D.J., Bass, J.D., Ringwood, A.E. and Sinclair, W. (1982) The single-crystal elastic moduli of stishovite. Journal of Geophysical Research, 87: 4740-4746.

Vita

Hui Zhao was born in Nanchang City, Jiangxi Province in China on June 20, 1965. He graduated with a B.Sc. degree from the department of applied mathematics at Chengdu College of Geology in 1989. In 1990, he came to Virginia Tech as a M.S. student. After four years of hard work, he finally finished his M.S. program and will go to Stony Brook to continue his Ph.D. work.